Neutral Guest Capture via Lewis Acid/Base Molecular Square Receptors. X-ray Crystal Structure of {Cyclobis[(*cis*-(dppp)Pt(4-ethynylpyridyl)$_2$)(*cis*- (PEt$_3$)$_2$Pt)]Ag$_2$}$^{+6}$(phenazine)-($^-$OSO$_2$CF$_3$)$_6$

Jeffery A. Whiteford and Peter J. Stang*

Department of Chemistry, University of Utah, Salt Lake City, Utah 84112

Songping D. Huang

Department of Chemistry, University of Puerto Rico, Rio Piedras, San Juan, Puerto Rico

Received June 24, 1998

Interaction of {cyclobis[(*cis*-(dppp)Pt(4-ethynylpyridyl)$_2$)(*cis*-(L)M)]Ag$_2$}$^{+6}$($^-$OSO$_2$CF$_3$)$_6$, where M = Pt(II) or Pd(II) and L = dppp or 2PEt$_3$, with pyridine, pyrazine, phenazine, or 4,4′-dipyridyl ketone results in coordination Lewis acid/base host−guest assemblies via the "π-tweezer effect" and mono or bis neutral guest coordination. All host−guest complexes are air stable microcrystalline solids with decomposition points greater than 170 °C. The homometallic Pt(II) receptors are more stable than the heteroaromatic Pt(II)−Pd(II) receptors toward heteratom-containing aromatic guests. The X-ray crystal structure of the host−guest complex {cyclobis[(*cis*-(dppp)Pt(4-ethynylpyridyl)$_2$)(*cis*-(PEt$_3$)$_2$Pt)]Ag$_2$}$^{+6}$(phenazine)($^-$OSO$_2$CF$_3$)$_6$ is reported. The crystals with the empirical formula $C_{62}H_{68}AgF_9N_3O_9P_4Pt_2S_3$ are triclinic $P\bar{1}$ with $a = 12.3919(8)$ Å, $b = 17.160(1)$ Å, $c = 18.932(1)$ Å, $\alpha = 90.892(1)°$, $\beta = 97.127(1)°$, $\gamma = 89.969(1)°$, and $Z = 2$.

Introduction

Intermolecular assembly by metal complexation is an important strategy for the preparation of a variety of synthetic receptors.[1−9] Recent examples include amine/Cu^{2+} hydrophobic sites,[1−3] hydroxylamine/Ni^{2+} alkali metal receptors,[4,5] a Tren derivative, [tris(aminoethyl)amine] functionalized with three *m*-hydroxyphenyl groups/Zn^{2+} trigonal bipyrimidal tripod,[6] and a bis(terpyridine) ruthenium(II) complex.[6] Benefits for both organic and inorganic substrates have been demonstrated by these synthetically designed binding sites such as lipophilic substrate binding, selective membrane cation transport, and transacylation rate acceleration, respectively.[1−6] Rigid systems utilizing porphyrin units designed by Sanders et al.[7] exploit metal coordination in two ways: (1) self-assembled Al^{3+} "activated" trispyridyl derivative guest; (2) self-assembled Pt(II)/tris-Lewis acid receptor Zn^{2+} site host. Interestingly, the self-assembled trispyridyl guest showed the highest affinity for the complementary porphyrin host when compared to covalent derivatives, demonstrated by association constant comparisons. Previous applications by Sanders et al.[8,9] showed how the acceleration of a pericyclic Diels Alder 4 + 2 reaction can be affected by "tuning" the binding site dimensions of rigid systems.

Site adaptability for receptor "tuning" via simple metal variation is a particularly attractive feature. Lang et al.[10,11] have shown that the "π-tweezer effect" via acetylene moieties is a viable option for cationic metal binding using Ti(IV) bistrimethylsilyl acetylene derivatives. We have recently shown that the "π-tweezer effect" can be incorporated in the arena of molecular squares, as verified by fast atom bombardment (FAB) mass spectrometry.[12−16] Molecular squares involving Lewis base receptor sites offer several advantages in design, such as (a) a variety of metal binding capabilities (Lewis acids: Ag(I), Au(I), Cu(I), Pd(II), Pt(II), etc.),[10−13,15,17] (b) geometrical predictability (enforced binding pocket dimensions between acetylenes), (c) binding energies between the range of the strong covalent bonding and weak hydrogen bonding, $\pi-\pi$ stacking, hydrophobic, and hydrophilic forces, or electrostatic interac-

(1) Scrimin, P.; Tecilla, P.; Tonelato, U.; Vignana, M. *J. Chem. Soc., Chem. Commun.* **1991**, 449−451.
(2) Schneider, H.-J.; Ruf, D. *Angew. Chem., Int. Ed. Engl.* **1990**, *29*, 1159−1160.
(3) Schneider, H.-J.; Blatter, T.; Zimmerman, P. *Angew. Chem., Int. Ed. Engl.* **1990**, *29*, 1161−1162.
(4) Schepartz, A.; McDevitt, J. P *J. Am. Chem. Soc.* **1989**, *111*, 5976−5977.
(5) Costes, J. P.; Dahan, F.; Laurent, J. P. *Inorg. Chem.* **1994**, *33*, 2738−2742.
(6) Linton, B.; Hamilton, A. D. *Chem. Rev.* **1997**, *97*, 1669−1680.
(7) Mackay, L. G.; Anderson, H. L.; Sanders, J. K. M. *J. Chem. Soc., Perkin Trans. 1* **1995**, 2269−2773.
(8) Bonar-Law, R. P.; Mackay, L. G.; Sanders, J. K. M. *J. Chem. Soc., Chem. Commun.* **1993**, 456−458.
(9) Walter, C. J.; Anderson, H. L.; Sanders, J. K. M. *J. Chem. Soc., Chem. Commun.* **1993**, 458−460.
(10) Back, S.; Pritzkow, H.; Lang, H. *Organometallics* **1998**, *17*, 41−44.
(11) Kohler, K.; Silverio, S. J.; Hyla-Krypspin, I.; Gleiter, R.; Zsolnai, L.; Driess, A.; Huttner, G.; Lang, H. *Organometallics* **1997**, *16*, 4970−4979.
(12) Manna, J.; Kuehl, C. J.; Whiteford, J. A.; Stang, P. J.; Muddiman, D. C.; Smith, R. D. *J. Am. Chem. Soc.* **1997**, *119*, 11611−11619.
(13) Whiteford, J. A. Self-Assembly and Host−Guest Chemistry of Cationic Titanium and Mixed, Neutral-Charged, Platinum(II) and Palladium(II) Macrocyclic Tetranuclear Complexes. Ph.D. Thesis, University of Utah, 1997; p 182.
(14) Manna, J.; Kuehl, C. J.; Whiteford, J. A.; Stang, P. J. *Organometallics* **1997**, *16*, 1897−1905.
(15) Whiteford, J. A.; Lu, C. V.; Stang, P. J. *J. Am. Chem. Soc.* **1997**, *119*, 2524−2533.
(16) Olenyuk, B.; Whiteford, J. A.; Stang, P. J. *J. Am. Chem. Soc.* **1996**, *118*, 8221−8230.

10.1021/ic980727c CCC: $15.00
Published on Web 09/24/1998

Scheme 1

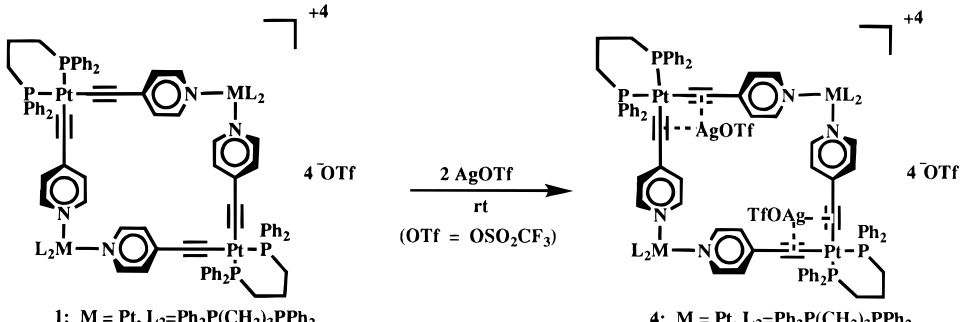

Scheme 2

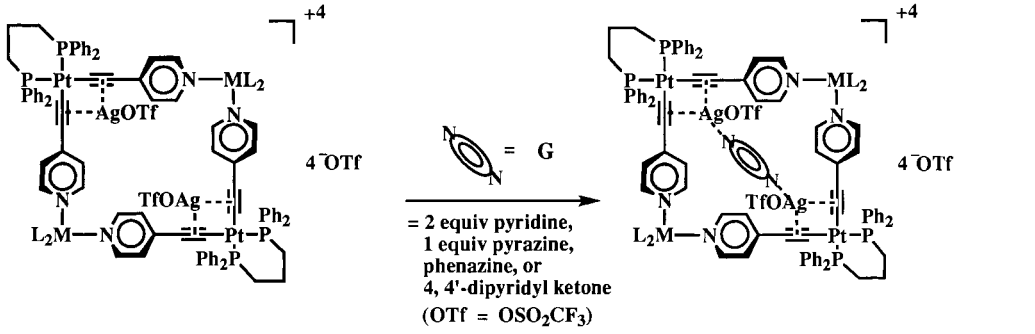

tions,[18] (d) excellent product yields due to self-assembly, and (e) multiple coordination sites for 3-D structure elaboration.[18]

In this paper, we wish to report (1) the first examples of molecular square/neutral guest coordination, (2) mono- and bis-coordinated neutral guests, (3) fast atom bombardment mass spectrometry (FABMS) spectra of a square/Ag complex, and (4) the X-ray crystal structure of cyclobis[[*cis*-Pt (dppp)(4-ethynylpyridine)$_2$][*cis*-Pt^{2+}(PEt$_3$)$_2$2$^-$OSO$_2$CF$_3$]]·2AgOTf·phenazine.

Results and Discussion

Interaction of 2 equiv of silver triflate between the acetylene moieties of molecular squares **1**−**3** resulted in host−guest complexes **4**−**6** (Scheme 1).[13,15] Receptors **4** and **6** are stable for months in the solid state and days in solution, whereas receptor **5** is stable for several weeks in solution and extended periods in the solid state. The order of increasing stability is **6** < **4** < **5**. Observation of the M/OTf base peak at 3447.6 amu for **5**, with isotopic distributions very close to the calculated patterns (+1 charge state), confirmed the 2:1 stoichiometry of the silver guest to the precursor square.[19] With a range of receptors, a series of guests could be used to determine the effects of neutral guest electron donation and their potential utility.

Coordinated, Neutral, Heteroatom, Aromatic Guests. Examination of cavity dimensions using Chem3D Plus, based on previous X-ray data,[15] revealed that guests possessing two heteroatoms, approximately 3 Å apart, should be of complementary size to coordinate to each respective silver cation. This seemed reasonable since ca. 3 Å are required between the neutral Pt center and the π-bonded metal cation (a total of 6 Å for C_2 symmetric complexes **4**−**6**).[10,11] The remaining 7 Å (out of a total of 13 Å for the diagonal distance of the square cavity) should allow sufficient space to accommodate the coordination of the bidentate guest heteroatom bonds to each of the respective cationic metals of complexes **4**−**6**. Indeed, reaction of Lewis acid/base receptor **4** with 2 equiv of pyridine or an equimolar amount of pyrazine, phenazine, or dipyridyl ketone, respectively, in CH_2Cl_2 at room temperature, results in the formation of host−guest complexes **7**−**10**, while reaction of **5** with pyrazine, phenazine, or dipyridyl ketone respectively, in acetone at room temperature, resulted in the formation of host−guest complexes **11**−**13** (Scheme 2). In a similar fashion, reaction of **6** with an equimolar amount of pyrazine or phenazine respectively, in acetone at room temperature, resulted in the formation of host−guest complexes **14** and **15**, all in excellent isolated yields (Scheme 2).

All nine host−guest complexes are stable microcrystalline solids with slight variation in coloration. Complexes **7**, **8**, **10**, **11**, and **13** are white, while complexes **9**, **12**, **14**, and **15** are light yellow. Host−guest complexes **7**−**10** are soluble in CH_2-

(17) Janssen, M. D.; Herres, M.; Zsolnai, L.; Spek, A. L.; Grove, D. M.; Lang, H.; van Koten, G. *Inorg. Chem.* **1996**, *35*, 2476−2483.
(18) Stang, P. J.; Olenyuk, B. *Acc. Chem. Res.* **1997**, *30*, 502−518.
(19) Whiteford, J. A.; Rachlin, E. M.; Stang, P. J. *Angew. Chem., Int. Ed. Engl.* **1996**, *35*, 2524−2529.

Cl_2, while complexes **11**−**15** are soluble in acetone and nitromethane.

The Lewis acid/base host−guest complexes have been fully characterized by analytical and spectral means as detailed in the Experimental Section. The $^{31}P\{^1H\}$ spectrum of **7** showed two singlets with a downfield shift of 1.4 ppm for the phosphorus on the neutral Pt (P−Pt); a 0.1 ppm upfield shift was observed for the phosphorus attached to the charged Pt (P−Pt^{2+}). The $^{31}P\{^1H\}$ spectra of **8**−**10** each show singlets with upfield shifts of 0.8−2.6 ppm for the phosphorus on the neutral Pt (P−Pt) and 3.1−3.9 ppm for the P−Pt^{2+} of **8**−**10**. The $^{31}P\{^1H\}$ spectra of **11**−**13** also show singlets with downfield shifts of 0.1−0.6 ppm for the phosphorus on the neutral Pt (P−Pt) and 0.01−0.2 ppm for the P−Pt^{2+} of **11**−**13**. The $^{31}P\{^1H\}$ spectra of **14** and **15** each show singlets with a downfield shift of 0.1−0.6 ppm for the phosphorus on the neutral Pt (P−Pt) and a 0.1−0.4 ppm upfield shift for the P−Pd^{2+} of **14** and **15**, respectively, relative to the precursors **4**−**6**. The increase or decrease in the Pt−P coupling for the phosphorus atoms on the neutral Pt ranged from −104 to +30 Hz, while the charged Pt corner differed from −3 to +13 Hz for **7**−**13**. The Pt−P coupling for the phosphorus atoms on the Pt−Pd systems **14** and **15** decreased by only 9 and 18 Hz, respectively, relative to precursors **4**−**6**. Equally important for the tetranuclear complexes **7**−**15** are the respective ^1H and $^{13}C\{^1H\}$ NMR spectra. The ^1H NMR signals for the methylenes of **7**−**10** for the charged metal-chelating dppp units and the methylenes of the neutral metal-chelating dppp units remain essentially unchanged, relative to the precursors **4**−**6**. Overlapping aromatic resonances were observed for the two sets of phenyl groups of the dppp ligand for **7**−**10**, while complexes **11**−**15** have signals for the methyl and methylene groups of the triethylphosphine ligands. The sets of aromatic resonances for the pyridyl unit (α and β to the pyridyl nitrogen) are doublets as expected. The α and β protons of the pyridyl resulted in small shifts of −0.25 to +0.01 ppm for **7**−**15**, upon coordination of heteroatom-containing neutral guests, while guest protons shifted from −0.48 to +0.10 ppm. Integration of the proton signals is in accord with the requirements for **7**−**15**. $^{13}C\{^1H\}$ NMR spectra of receptor complexes each show overall downfield shifts in the dppp phenyl ring carbons as well as in the ethyl group carbons of the triphenylphosphine ligands. The most significant ^{13}C shifts were observed for the pyridyl ipso carbon and the alkyne β-carbon of the ethynyl pyridine ligands (−0.2 to +2.8 ppm). Guest carbon atoms shifted downfield upon coordination, ranging from 0.1 to 12.3 ppm. The IR spectra of the complexes were equally interesting. Remarkably, upon coordination of heteroatomic guests, the alkyne stretch shifts appear inconsistent. The transfer of electron density from the neutral guest into the π-coordinated metal resulted in a shift to higher wavenumbers for **8**, **9**, and **13**, while **7**, **10**−**12**, **14**, and **15** shifted to lower wavenumbers. One would expect a trend of IR shifts related to the difference in guest electronics.[17] However, this is not the case for host−guest complexes **7**−**15**. The phenyl rings of the dppp ligands may be partially responsible for this anomaly (see X-ray section for details). The ^{19}F spectra for **7**−**15** display singlets from −75 to −76 ppm, characteristic for ionic $CF_3SO_3^-$.

Single-Crystal X-ray Molecular Structure Determination. The geometrical features of molecular squares, as determined through X-ray crystallography, provided insight for adaptation toward molecular receptor design.[13,15,20,21] Continued progress in design variation of these macrocycles has proven useful for the determination of host−guest interactions and convergent binding sight construction. Bond angles and cavity size were important features for the determination of potential guest size and dimension. Therefore, we attempted to obtain X-ray quality crystals of all macrocyclic squares. Unfortunately, the crystals of all macrocycles described are solvent dependent, due to extensive solvent occlusion in their cavities, and collapse into amorphous material upon removal from the mother liquor. Previously, only the precursor for complex **6** gave single crystals suitable for X-ray determination. This crystallographic data was the basis for the selection of appropriately sized, heteroatom-containing guests. Subsequent binding of the guest phenazine to the π-bonded Ag^+ atoms resulted in complex **12**. The twofold benefit of macrocycle torsional stability and void space reduction were most likely responsible for stabilizing the crystal lattice of **12**. The numbering diagram, ORTEP representation, and significant geometric features are shown in Figure 1. The crystal and structure refinement data are given in Table 1. Selected key bond distances and angles are given in Table 2. A side view ORTEP representation generated with ORTEP-3 for Windows is provided to show important framework features and the orientation of the Ag^+ atoms with respect to the Pt−Pt^{2+}−Pt plane and guest proximity (Figure 2).

There are several interesting structural features evident for complex **12.** The overall geometry of the perimeter for complex **12** is nearly planar with the guest phenazine oriented nearly orthogonal to the Pt−Pt^{2+}−Pt plane. The π-complexed silver atoms are located in a pseudotrans arrangement with respect to the Pt−Pt^{2+}−Pt plane, resulting in a C_i-symmetric relationship. This is probably a result of the distance between guest heteroatoms being slightly larger than needed for optimal guest fit. The bonding geometry for the neutral Pt and Pt^{2+} centers is square planar but with small deviation from the expected 90° angles. The P−Pt−P angle is 93.0°, whereas the silver-coordinated C−Pt−C angle increased from 88° to 89.5° upon Lewis acid/base complexation.[15] The N−Pd−N bond angle for macrocycle **3** is 85.0°, whereas the N−Pt−N bond angle for **12** is 84.2°. Although the "bite-angle" usually decreases upon metal coordination in titanium bis-ethynyl monomers, as reported by Lang et al.,[10,11,17] the presumably smaller starting angle of complex **5** required a "bite-angle" increase to accommodate the silver and neutral guest. The edge-to-edge Pt−Pt^{2+} distance is 9.50 Å, the diagonal Pt−Pt distance is 13.7 Å, and the diagonal Pt^{2+}−Pt^{2+} distance is 13.2 Å. While the distance from the neutral Pt to Ag is 3.32 Å, the distance between the coordinated phenazine nitrogen and the π-bound Ag^+ is 2.31 Å. The distance between the two π-coordinated silver atoms is 7.41 Å, and the distance between the phenazine nitrogens is 2.84 Å. Examination of the space-filling model of **12**, which is based upon the X-ray data, reveals a more realistic view of host−guest fit by including the calculated atomic radii representation. Very little space is left available upon phenazine inclusion. Consequently, no solvent molecules were located in host−guest complex **12**, unlike in the precursor to **6**, where five solvent molecules were reported in the crystal lattice. The 4-ethynyl pyridine ligands of **12** are bent slightly inward toward the center of the complex. The pyridyl ligands are nearly orthogonal to the plane defined by the dppp ligand and do not display π−π interaction with the phenyl rings of the dppp subunit as seen with the cationic square crystal structures previously reported.[13,15,20,21] However, the alkyne units apparently interact with the dppp phenyl rings as evidenced by the

(20) Stang, P. J.; Chen, K.; Arif, A. M. *J. Am. Chem. Soc.* **1995**, *117*, 8793−8797.

(21) Stang, P. J.; Cao, D. H.; Saito, S.; Arif, A. M. *J. Am. Chem. Soc.* **1995**, *117*, 6273−6283.

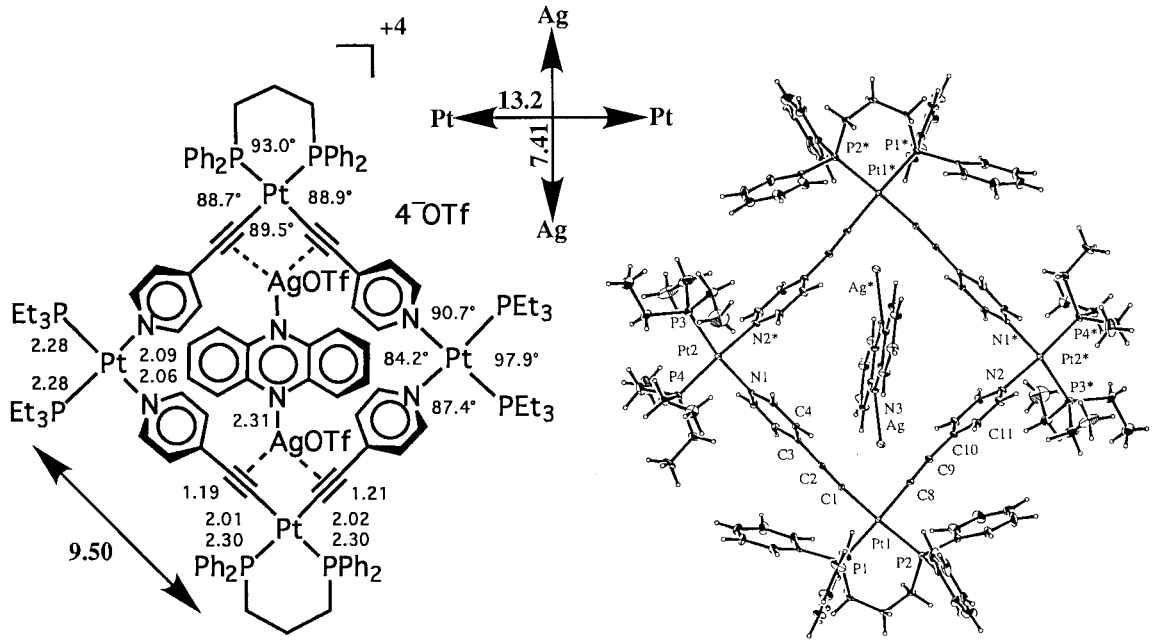

Figure 1. ORTEP representation (35% ellipsoids) and summary of the significant geometric features of host−guest complex **12** (bond lengths are in angstroms, OTf = OSO_2CF_3).

Table 1. Crystallographic Data for **12**

chemical formula	$C_{62}H_{68}AgF_9N_3O_9P_4Pt_2S_3$
fw	1888.34
a, Å	12.3919(8)
b, Å	17.160(1)
c, Å	18.932(1)
α, deg	90.892(1)
β, deg	97.127(1)
γ, deg	89.969(1)
V, Å^3	3987.3(4)
Z	2
space group	$P\bar{1}$ (no. 2)
T, °C	23
λ, Å	0.7107
ρ (calcd), g/m^3	1.573
μ, cm^{-1}	0.3956
R (%)[a]	5.20
R_w (%)[b]	7.30

[a] $R = \sum(|F_o| - |F_c|)/\sum|F_o|$. [b] $R_w = [\sum_w(|F_o| - |F_c|)^2/\sum_w|F_o|^2]^{1/2}$, $w = 1/\sigma^2(F)$.

orientation change upon silver and subsequent neutral guest coordination, shown by comparing the X-ray crystal structure of the precursor of **6** to **12**.[13,15] This may be responsible for the unusual behavior of the IR alkyne stretch trends as well as the ^{31}P coupling constant differences.[22,23] The M−P distances (2.28 Å) are normal and similar to distances obtained earlier on uncomplexed macrocyclic squares. Likewise the M−N distances (2.06 and 2.09 Å) are normal and similar to distances on macrocyclic squares previously reported.[13,15,20,21] The M−alkyne bond lengths are 2.01 and 2.02 Å, and the C≡C alkyne bond lengths are 1.19 and 1.21 Å for **12**, which differ very little from those for the precursor to **6**. The alkyne−pyridyl−ipso carbon bond lengths are 1.47 and 1.44 Å very close to all other metal/alkyne complexes[24−26]

Table 2. Selected Bond Lengths [Å] and Angles [deg] for Host−Guest Complex **12**

Bond Distances			
Pt(1)−C(1)	2.01(1)	P(3)−C(42)	1.84(2)
Pt(1)−C(8)	2.02(1)	P(3)−C(44)	1.79(3)
Pt(2)−P(3)	2.276(5)	P(3)−C(46)	1.78(2)
Pt(2)−P(4)	2.277(4)	P(4)−C(48)	1.78(2)
Pt(2)−N(1)	2.06(1)	P(4)−C(50)	1.80(2)
Pt(2)−N(2)	2.09(1)	P(4)−C(52)	1.83(2)
Ag−N(3)	2.31(1)	Ag−C(8)	2.45(1)
P(1)−C(21)	1.85(1)	C(1)−C(2)	1.19(2)
P(1)−C(27)	1.84(1)	C(2)−C(3)	1.47(2)
P(2)−C(29)	1.82(1)	C(3)−C(4)	1.43(2)
C(8)−C(9)	1.21(2)	C(9)−C(10)	1.44(2)
Bond Angles			
P(1)−Pt(1)−P(2)	93.0(1)	Pt(1)−C(1)−C(2)	174(1)
P(1)−Pt(1)−C(1)	88.9(4)	C(1)−C(2)−C(3)	179(2)
P(1)−Pt(1)−C(8)	177.1(4)	C(2)−C(3)−C(4)	121(1)
P(2)−Pt(1)−C(1)	177.8(4)	C(2)−C(3)−C(7)	124(1)
P(2)−Pt(1)−C(8)	88.7(4)	C(4)−C(3)−C(7)	116(1)
C(1)−Pt(1)−C(8)	89.4(5)	C(3)−C(4)−C(5)	120(1)
P(3)−Pt(2)−P(4)	97.9(2)	N(1)−C(5)−C(4)	123(1)
P(3)−Pt(2)−N(1)	170.7(3)	N(1)−C(6)−C(7)	124(1)
P(3)−Pt(2)−N(2)	87.4(3)	Pt(1)−C(8)−Ag	95.4(6)
P(4)−Pt(2)−N(1)	90.7(3)	Pt(1)−C(8)−C(9)	179(1)
P(4)−Pt(2)−N(2)	174.1(3)	Ag−C(8)−C(9)	83(1)
N(1)−Pt(2)−N(2)	84.2(4)	C(8)−C(9)−C(10)	172(2)
N(3)−Ag−C(8)	118.3(5)	C(9)−C(10)−C(11)	124(1)

The stacking pattern of **12** in the solid state revealed that the host−guest complexes are stacked along the *B*-axis, with each guest stacked over the next, aligning the intercomplementary phenazine ring system electronics.[27−30] The channel-like cavity

(22) Wrackmeyer, B.; Horchler, K. *Progress in NMR Spectroscopy*: *NMR Parameters of Alkynes*; Pergamon Press: Great Britain, 1990; pp 209−253.
(23) Morris, D. G. In *The Chemistry of Functional Groups, Supplement C*: *NMR Spectra of Acetylenes*; Patai, S., Rappoport, Z., Eds.; John Wiley & Sons Ltd.: New York, 1983; pp 1035−1056.
(24) Manna, J.; John, K. D.; Hopkins, M. D. *Adv. Organomet. Chem.* **1995**, *38*, 79−154 and references therein.
(25) Berenguer, J. R.; Forniés, J.; Lalinde, E.; Martínez, F. *J. Organomet. Chem.* **1994**, *470*, C15−C18.
(26) Wisner, J. M.; Bartczak, T. J.; Ibers, J. A.; Low, J. J.; Goddard, W. A., III *J. Am. Chem. Soc.* **1986**, *108*, 347−348.
(27) Dunitz, J. D. In *Perspectives In Supramolecular Chemistry*, *The Crystal as a Supramolecular Entity: Thoughts on Crystals as Supermolecules*; Desiraju, G. R.; Ed., John Wiley & Sons Ltd.: West Sussex, England, 1996; pp 1−30.
(28) Chen, C.-T.; Chadha, R.; Siegel, J. S.; Hardcastle, K. *Tetrahedron Lett.* **1995**, *36*, 8403−8406.

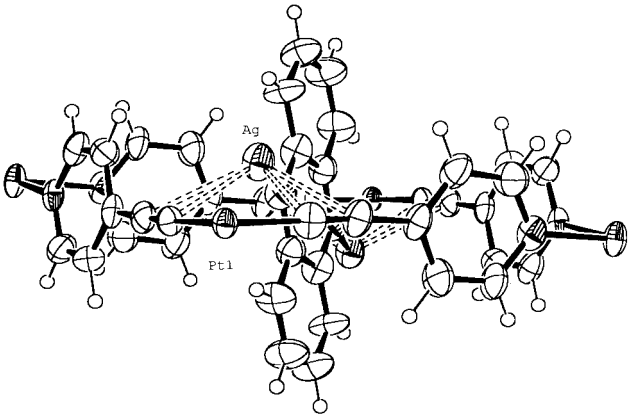

Figure 2. Side view of host−complex **12**.

formed by the molecular square frame contains little void space with the inclusion of the cationic silver atoms and the neutral guest. The repeating unit distance between each stacked host−guest complex is ca. 17.2 Å, which is larger than the hybrid-iodonium−transition metal[20] and Pt−Pd ethynyl pyridine square[15] distance at 9.5 and 10.7 Å, respectively, and the nonplanar all transition metal 4,4′-bipyridine square[21] distance at 15.9 Å. The six triflate counterions are ordered, with two triflate counterions located near each of the charged Pt corners (a total of four), while the remaining two triflates are in close proximity to the silver atoms (one per silver atom).

Conclusions

A total of nine novel homo- and heteronuclear mixed neutral-charged organometallic host−guest complexes were synthesized via modular self-assembly featuring 4-ethynylpyridine ligands with two types of Pt and Pd phosphine ligands (dppp and triethylphoshine). Each host−guest precursor contains silver coordinated via the "π-tweezer effect" between each respective set of acetylene moieties. Four different neutral guests were subsequently coordinated to the cationic silver metal via mono- or bidentate heteroatom electron dative bonding. The Pt−Pd heteronuclear square-based host−guest complexes **14** and **15** are significantly less stable than the Pt−Pt homonuclear square-based host−guest complexes **7**−**13**. The most stable complex resulted from Lewis acid/base receptor **5** and the neutral guest phenazine, while the least stable complex resulted from receptor **6** and dipyridyl ketone. The Lewis acid/base, molecular square receptors incorporating acetylene groups and silver cations readily bind neutral guests such as pyridine, pyrazine, phenazine, and dipyridyl ketone. The addition of the respective guest to the 4-ethynylpyridine-based Pt−Pt/Ag^+ and Pt−Pd/Ag^+ receptors clearly shows host−guest interaction via the "π-tweezer effect" and heteroatom coordination. Significant shift values in the ^{31}P, ^{1}H, ^{13}C NMR, and IR spectra support the proposed inclusion phenomenon. The X-ray crystal structure of **12** confirmed the 1:1 stoichiometry of the Lewis acid/base receptor/neutral phenazine guest complex. These geometric and stability data represent an important step toward the development of artificial receptors.

Experimental Section

General Methods. Melting points (uncorrected) were obtained with a Mel-Temp capillary melting point apparatus. Infrared spectra were recorded as CCl_4 mulls on a Mattson FT-IR spectrometer. All NMR spectra were recorded on a Varian Unity 300 or a Varian VXR 500 spectrometer. The ^{1}H NMR spectra were recorded at 300 MHz, and chemical shifts are reported relative to the residual protonated solvent peaks of CD_2Cl_2 δ 5.32 and acetone-d_6 δ 2.05. The ^{13}C NMR spectra were recorded at 75 or 125 MHz, ^{1}H decoupled, and reported relative to CD_2Cl_2 δ 54.0 or acetone-d_6 δ 29.93. The ^{19}F NMR spectra were recorded at 282 MHz, and chemical shifts were reported relative to external $CFCl_3$ δ 0.0 (sealed capillary). The ^{31}P NMR spectra were recorded at 121 MHz, ^{1}H decoupled, and reported relative to external 85% H_3PO_4 (sealed capillary).

Mass spectra were obtained with a Finnigan MAT 95 mass spectrometer with a Finnigan MAT ICIS II operating system under positive fast atom bombardment (FAB) conditions at 8 keV. 3-Nitrobenzyl alcohol was used as a matrix in acetone as the solvent; polypropylene glycol and cesium iodide were used as a reference for peak matching. Microanalyses were performed by Atlantic Microlabs, Atlanta, GA.

Materials. All commercial reagents were ACS reagent grade and used without further purification or after sublimation. Reagent grade methylene chloride was dried by distillation over CaH_2. Diethyl ether and THF were distilled from Na/benzophenone. Acetone was refluxed over $KMnO_4$, distilled, and handled under nitrogen. HPLC grade benzene, toluene, and pentane were dried over molecular sieves and used without further purification. Reaction flasks were flame-dried and flushed with argon prior to use with Schlenk techniques unless otherwise noted. Trimethylsilyl acetylene, diphenylphosphinopropane, silver triflate, 2.5 M *n*-butyllithium in hexanes, and 1.7 M *tert*-butyllithium in pentane were purchased from Aldrich. Pd(II) dichloride was purchased from Lancaster.

{Cyclobis[(*cis*-(dppp)Pt(4-ethynylpyridyl)$_2$)(*cis*-(PEt$_3$)$_2$Pt)]Ag$_2$}$^{+6}$-($^{-}$OSO$_2$CF$_3$)$_6$ Complex (5). To a solution of square **2**[15] in 750 μL of acetone-d_6 in a 5 mm NMR tube (25.6 mg, 0.00830 mmol) was added 2.0 equiv (4.3 mg, 0.0166 mmol) of AgOTf in one portion at 25 °C; then the reaction mixture was shaken. The solvent was removed under a stream of nitrogen at room temperature followed by solvent removal in vacuo, resulting in a white microcrystalline solid (29.6 mg, 99%): mp 298−303 °C dec; IR (CCl_4) 3055, 3095 (Ar), 2933 (CH_2), 2091 (CC), 1259, 1151, 1103, 1029 (OTf) cm^{-1}; ^{1}H NMR (acetone-d_6) δ 8.78 (d, 8H, $^{3}J_{HH}$ = 5.6 Hz), 7.72−7.63 (m, 16H, *o*), 7.47−7.37 (m, 24H, *m*, *p*), 6.86 (d, 8H, $^{3}J_{HH}$ = 6.0 Hz), 3.02 (bs, 8H), 2.10−1.80 (obscured, m, 8H), 2.00−1.85 (m, 24H), 1.40−1.24 (m, 36H); ^{13}C-{^{1}H} NMR (acetone-d_6) δ 134.3 (Pt−P−C$_o$), 130.1 (Pt−P−C$_{ipso}$), 132.3 (Pt−P−C$_p$), 129.7 (Pt−P−C$_m$), 150.3 (C$_{\alpha pyr}$), 129.8 (C$_{\beta pyr}$), 137.7 (C$_{ipsopyr}$), 109.1 (t, CC−Pt$_\beta$), 122.2 (q, J_{C-F} = 321 Hz, OTf), 23.9 (m, Pt−P−CH$_2$), 19.7 (bs, CH$_2$), 15.5 (m, Pt−P−*C*H$_2$CH$_3$), 8.2 (bs, Pt−P−CH$_2$*C*H$_3$); ^{31}P{^{1}H} NMR (acetone-d_6) δ 3.6 (s, J_{Pt-P} = 3073 Hz), −4.7 (s, J_{Pt-P} = 2324 Hz);^{19}F NMR (CD_2Cl_2) δ −75; FAB LRMS, *m*/*z* 3447.6 (M − OTf).

{Cyclobis[(*cis*-(dppp)Pt(4-ethynylpyridyl)$_2$)(*cis*-(dppp)Pt)]Ag$_2$}$^{+6}$-(pyridyl)$_2$($^{-}$OSO$_2$CF$_3$)$_6$ Complex (7). To a solution of silver triflate complex **4**[15] in 750 μL of CD_2Cl_2 in a 5 mm NMR tube (20.2 mg, 0.0051 mmol) was added 2 equiv (0.811 mg, 0.829 μL, 0.0103 mmol) of pyridine in one portion at 25 °C via syringe; then the reaction mixture was shaken. The solvent was removed under a stream of nitrogen at room temperature followed by solvent removal in vacuo, resulting in a white microcrystalline solid (20.8 mg, 99%): mp 198−202 °C dec; IR (CCl_4) 3056, 3097 (Ar), 2927 (CH_2), 2080 (CC), 1253, 1154, 1103, 1027 (OTf) cm^{-1}; ^{1}H NMR (CD_2Cl_2) δ 8.32 (d, 8H, $^{3}J_{HH}$ = 5.1 Hz), 8.14 (d, 4H, $^{3}J_{HH}$ = 4.5 Hz, pyridine-*o*), 7.85 (t, 4H, $^{3}J_{HH}$ = 7.8 Hz, pyridine-*p*), 7.85 (dd, 4H, $^{3}J_{HH}$ = 6.0 Hz, pyridine-*m*), 7.70−7.16 (m, 80H), 6.19 (d, 8H, $^{3}J_{HH}$ = 6.0 Hz), 3.17 (bs, 8H), 2.62 (bs, 8H), 2.13 (m, 8H); ^{13}C{^{1}H} NMR (CD_2Cl_2) δ 134.0 (Pt−P−C$_o$), 129.6 (Pt−P−C$_{ipso}$), 132.8 (Pt−P−C$_p$), 129.9 (Pt−P−C$_m$), 133.7 (Pt′−P−C$_o$), 132.2 (Pt′−P−C$_p$), 129.8 (Pt′−P−C$_m$), 125.0 (Pt′−P−C$_{ipso}$), 149.6 (C$_{\alpha pyr}$), 129.4 (C$_{\beta pyr}$), 138.2 (C$_{ipsopyr}$), 151.3 (pyridine$_o$), 139.8 (pyridine$_p$), 127.2 (pyridine$_m$), 121.7 (q, J_{C-F} = 321 Hz, OTf), 108.3 (t, CC−Pt$_\beta$), 25.3 (Pt−P−CH$_2$), 21.9 (Pt′−P−CH$_2$), 19.8 (CH$_2$), 18.2 (CH′$_2$); ^{31}P{^{1}H} NMR (CD_2Cl_2) δ −4.8 (s, J_{Pt-P} = 2334 Hz), −11.2 (s, J_{Pt-P} = 3062 Hz); ^{19}F NMR (CD_2Cl_2) δ −75. Anal. Calcd for $Pt_4Ag_2C_{152}H_{130}P_8S_6N_6O_{18}F_{18}$: C, 44.45; H, 3.19; N, 2.05; S, 4.68. Found: C, 44.77; H, 3.35; N, 2.17; S, 4.77.

(29) Cozzi, F.; Ponzini, F.; Annunziata, R.; Cinquini, M.; Siegel, J. S. *Angew. Chem., Int. Ed. Engl.* **1995**, *34*, 1019−1020.
(30) Cozzi, F.; Siegel, J. S. *Pure Appl. Chem.* **1995**, *67*, 683−689.

{Cyclobis[(*cis*-(dppp)Pt(4-ethynylpyridyl)$_2$)(*cis*-(dppp)Pt)]Ag$_2$}$^{+6}$-(pyrazine)($^-$OSO$_2$CF$_3$)$_6$ Complex (8). To a solution of silver triflate complex **4**[15] in 750 μL of CD_2Cl_2 in a 5 mm NMR tube (25.6 mg, 0.0065 mmol) was added 1 equiv (0.520 mg, 0.0065 mmol) of pyrazine in one portion at 25 °C; then the reaction mixture was shaken. The solvent was removed under a stream of nitrogen at room temperature followed by solvent removal in vacuo, resulting in a white microcrystalline solid (26.2 mg, 99%): mp 242−245 °C dec; IR (CCl_4) 3057, 3097 (Ar), 2938 (CH_2), 2117 (CC), 1252, 1159, 1102, 1029 (OTf) cm^{-1}; ^{1}H NMR (CD_2Cl_2) δ 8.50 (pyrazine bs, 4H), 8.25 (d, 8H, $^3J_{HH}$ = 3.9 Hz), 7.70−7.16 (m, 80H), 6.26 (d, 8H, $^3J_{HH}$ = 6.4 Hz), 3.15 (bs, 8H), 2.55 (bs, 8H), 2.09 (m, 8H); ^{13}C{^{1}H} NMR (CD_2Cl_2) δ 133.9 (Pt−P−C$_o$), 130.0 (Pt−P−C$_{ipso}$), 132.6 (Pt−P−C$_p$), 129.7 (Pt−P−C$_m$), 133.5 (Pt′−P−C$_o$), 132.0 (Pt′−P−C$_p$), 129.3 (Pt′−P−C$_m$), 125.1 (Pt′−P−C$_{ipso}$), 149.4 (C$_{\alpha pyr}$), 128.3 (C$_{\beta pyr}$), 135.2 (C$_{ipsopyr}$), 145.8 (pyrazine), 121.7 (q, J_{C-F} = 321 Hz, OTf), 25.9 (Pt−P−CH_2), 21.8 (Pt′−P−CH_2), 20.5 (CH_2), 18.2 (CH'_2); ^{31}P{^{1}H} NMR (CD_2Cl_2) δ −7.0 (s, J_{Pt-P} = 2251 Hz), −14.5 (s, J_{Pt-P} = 3058 Hz); ^{19}F NMR (CD_2Cl_2) δ −75.

{Cyclobis[(*cis*-(dppp)Pt(4-ethynylpyridyl)$_2$)(*cis*-(dppp)Pt)]Ag$_2$}$^{+6}$-(phenazine)($^-$OSO$_2$CF$_3$)$_6$ Complex (9). To a solution of silver triflate complex **4**[15] in 750 μL of CD_2Cl_2 in a 5 mm NMR tube (24.9 mg, 0.0063 mmol) was added 1 equiv (1.14 mg, 0.0063 mmol) of phenazine in one portion at 25 °C; then the reaction mixture was shaken. The solvent was removed under a stream of nitrogen at room temperature followed by solvent removal in vacuo, resulting in a yellow microcrystalline solid (25.8 mg, 99%): mp 250−253 °C dec; IR (CCl_4) 3057, 3094 (Ar), 2917 (CH_2), 2088 (CC), 1252, 1155, 1105, 1028 (OTf) cm^{-1}; ^{1}H NMR (CD_2Cl_2) δ 8.32−8.13 (m, 4H, phenazine-β), 8.32−8.18 (d, 8H), 7.81 (m, 4H, phenazine-γ), 7.70−7.16 (m, 80H), 6.23 (d, 8H), 3.10 (bs, 8H), 2.76 (bs, 8H), 2.11 (m, 8H); ^{13}C{^{1}H} NMR (CD_2Cl_2) δ 133.4 (Pt−P−C$_o$), 130.7 (Pt−P−C$_{ipso}$), 132.1 (Pt−P−C$_p$), 129.2 (Pt−P−C$_m$), 134.0 (Pt′−P−C$_o$), 132.6 (Pt′−P−C$_p$), 129.7 (Pt′−P−C$_m$), 124.9 (Pt′−P−C$_{ipso}$), 149.5 (C$_{\alpha pyr}$), 128.6 (C$_{\beta pyr}$), 135.4 (C$_{ipsopyr}$), 143.2 (phenazine-α), 132.7 (phenazine-β), 129.5 (phenazine-γ), 122.8 (q, CC−Pt$_\alpha$), 121.5 (q, J_{C-F} = 321 Hz, OTf), 111.9 (t, CC−Pt$_\beta$), 24.5 (Pt−P−CH_2), 21.9 (Pt′−P−CH_2), 19.9 (CH_2), 18.1 (CH'_2); ^{31}P{^{1}H} NMR (CD_2Cl_2) δ −8.8 (s, J_{Pt-P} = 2385 Hz), −15.0 (s, J_{Pt-P} = 3070 Hz); ^{19}F NMR (CD_2Cl_2) δ −75.

{Cyclobis[(*cis*-(dppp)Pt(4-ethynylpyridyl)$_2$)(*cis*-(dppp)Pt)]Ag$_2$}$^{+6}$-(4,4′-dipyridylketone)($^-$OSO$_2$CF$_3$)$_6$ Complex (10). To a solution of silver triflate complex **5** in 750 μL of CD_2Cl_2 in a 5 mm NMR tube (21.5 mg, 0.0055 mmol) was added 1 equiv (1.00 mg, 0.0055 mmol) of 4,4′-dipyridyl ketone in one portion at 25 °C; then the reaction mixture was shaken. The solvent was removed under a stream of nitrogen at room temperature followed by solvent removal in vacuo, resulting in an orange solid (22.4 mg, 99%): mp 215−218 °C dec; IR (CCl_4) 3055, 3098 (Ar), 2925 (CH_2), 2080 (CC), 1253, 1154, 1102, 1027 (OTf) cm^{-1}; ^{1}H NMR (CD_2Cl_2) δ 8.66 (d, 4H, dipyridyl ketone-pyr-α), 8.29 (d, 8H), 7.80−7.15 (m, 80H), 7.10 (d, 4H, dipyridyl ketone-pyr-β), 6.14 (d, 8H), 3.17 (bs, 8H), 2.69 (bs, 8H), 2.12 (m, 8H); ^{13}C{^{1}H} NMR (CD_2Cl_2) δ 133.7 (Pt−P−C$_o$), 129.9 (Pt−P−C$_{ipso}$), 132.6 (Pt−P−C$_p$), 129.8 (Pt−P−C$_m$), 133.2 (Pt′−P−C$_o$), 132.4 (Pt′−P−C$_p$), 129.6 (Pt′−P−C$_m$), 125.5 (Pt′−P−C$_{ipso}$), 149.4 (C$_{\alpha pyr}$), 129.5 (C$_{\beta pyr}$), 135.9 (C$_{ipsopyr}$), 207.0 (dipyridyl ketone-CO), 152.2 (dipyridyl ketone-pyr-α), 145.0 (dipyridyl ketone-pyr-ipso), 127.1 (dipyridyl ketone-pyr-β), 121.5 (q, J_{C-F} = 321 Hz, OTf), 109.1 (CC$_\beta$), 25.1 (Pt−P−CH_2), 22.0 (Pt′−P−CH_2), 19.9 (CH_2), 18.1 (CH'_2); ^{31}P{^{1}H} NMR (CD_2Cl_2) δ −8.1 (s, J_{Pt-P} = 2338 Hz), −14.2 (s, J_{Pt-P} = 3054 Hz); ^{19}F NMR (CD_2Cl_2) δ −76. Anal. Calcd for $Pt_4Ag_2C_{153}H_{128}P_8S_6N_6O_{19}F_{18}$·$CD_2Cl_2$: C, 43.83; H, 3.15; N, 1.99; S, 4.56. Found: C, 43.87; H, 3.30; N, 2.19; S, 4.80.

{Cyclobis[(*cis*-(dppp)Pt(4-ethynylpyridyl)$_2$)(*cis*-(PEt$_3$)$_2$Pt)]Ag$_2$}$^{+6}$-(pyrazine)($^-$OSO$_2$CF$_3$)$_6$ Complex (11). To a solution of silver triflate complex **5** in 750 μL of acetone-d_6 in a 5 mm NMR tube (39.0 mg, 0.0109 mmol) was added 1 equiv (0.870 mg, 0.0109 mmol) of pyrazine in one portion at 25 °C; then the reaction mixture was shaken. The solvent was removed under a stream of nitrogen at room temperature followed by solvent removal in vacuo to give the product compound (39.8 mg, 99%): mp 225−228 °C dec; IR (CCl_4) 3056, 3099 (Ar), 2938 (CH_2), 2078 (CC), 1257, 1157, 1105, 1028 (OTf) cm^{-1}; ^{1}H NMR (acetone-d_6) δ 8.71 (d, 8H, $^3J_{HH}$ = 3.0 Hz), 8.54 (s, 4H, pyrazine), 7.80−7.65 (m, 16H, *o*), 7.50−7.36 (m, 24H, *m*, *p*), 6.87 (d, 8H, $^3J_{HH}$ = 6.4 Hz), 3.09 (bs, 8H), 2.25−1.85 (m, 8H), 1.95−1.80 (m, 24H), 1.35−1.20 (m, 36H); ^{13}C{^{1}H} NMR (acetone-d_6) δ 134.4 (Pt−P−C$_o$), 130.0 (Pt−P−C$_{ipso}$), 132.4 (Pt−P−C$_p$), 129.7 (Pt−P−C$_m$), 150.6 (C$_{\alpha pyr}$), 129.5 (C$_{\beta pyr}$), 137.0 (C$_{ipsopyr}$), 146.8 (pyrazine) 109.6 (t, $^2J_{P-C}$ = 22.4 Hz, CC−Pt$_\beta$), 122.3 (q, J_{C-F} = 321 Hz, OTf), 23.4 (m, Pt−P−CH_2), 19.7 (bs, CH_2), 15.4 (m, Pt−P−CH_2CH_3), 8.2 (bs, Pt−P−CH_2CH_3); ^{31}P{^{1}H} NMR (acetone-d_6) δ 3.8 (s, J_{Pt-P} = 3073 Hz), −4.6 (s, J_{Pt-P} = 2338 Hz); ^{19}F NMR (CD_2Cl_2) δ −75. Anal. Calcd for $Pt_4Ag_2C_{116}H_{132}P_8S_6N_6O_{18}F_{18}$·$OC(CD_3)_2$: C, 38.21; H, 3.88; N, 2.25; S, 5.14. Found: C, 38.40; H, 3.79; N, 2.40; S, 5.54.

{Cyclobis[(*cis*-(dppp)Pt(4-ethynylpyridyl)$_2$)(*cis*-(PEt$_3$)$_2$Pt)]Ag$_2$}$^{+6}$-(phenazine)($^-$OSO$_2$CF$_3$)$_6$ Complex (12). To a solution of silver triflate complex **5** in 750 μL of acetone-d_6 in a 5 mm NMR tube (38.8 mg, 0.0108 mmol) was added 1 equiv (1.94 mg, 0.0108 mmol) of phenazine in one portion at 25 °C; then the reaction mixture was shaken. The solvent was removed under a stream of nitrogen at room temperature followed by solvent removal in vacuo, resulting in a yellow microcrystalline solid (40.5 mg, 99%): mp 230−234 °C dec. X-ray quality crystals were obtained by preparing a saturated (0.0154 M) solution (in a nitrogen atmosphere glovebag) in acetone-d_6 in a 5 mm NMR tube and allowing it to crystallize at room temperature overnight: IR (CCl_4) 3056, 3097 (Ar), 2933 (CH_2), 2083 (CC), 1259, 1155, 1105, 1028 (OTf) cm^{-1}; ^{1}H NMR (acetone-d_6) δ 8.52 (d, 8H, $^3J_{HH}$ = 3.1 Hz), 8.45 (m, 4H $^3J_{HH}$ = 10.3 Hz, phenazine-β), 7.97 (m, 4H $^3J_{HH}$ = 10.3 Hz, phenazine-γ), 7.80−7.65 (m, 16H, *o*), 7.41−7.35 (m, 24H, *m*, *p*), 6.79 (d, 8H, $^3J_{HH}$ = 6.4 Hz), 3.07 (bs, 8H), 2.15−1.85 (m, 8H), 1.95−1.85 (m, 24H), 1.40−1.15 (m, 36H); ^{13}C{^{1}H} NMR (acetone-d_6) δ 134.4 (Pt−P−C*o*), 130.3 (Pt−P−C$_{ipso}$), 132.2 (Pt−P−C$_p$), 129.6 (Pt−P−C$_m$), 150.3 (C$_{\alpha pyr}$), 129.3 (C$_{\beta pyr}$), 144.0 (phenazine-α), 132.9 (phenazine-β), 129.2 (phenazine-γ), 109.9 (t, CC−Pt$_\beta$), 122.3 (q, J_{C-F} = 321 Hz, OTf), 23.8 (m, Pt−P−CH_2), 19.8 (bs, CH_2), 15.4 (m, Pt−P−CH_2CH_3), 8.1 (bs, Pt−P−CH_2CH_3); ^{31}P{^{1}H} NMR (acetone-d_6) δ 3.6 (s, J_{Pt-P} = 3071 Hz), −4.1 (s, J_{Pt-P} = 2318 Hz);^{19}F NMR (CD_2Cl_2) δ −75. Anal. Calcd for $Pt_4Ag_2C_{124}H_{136}P_8S_6N_6O_{18}F_{18}$: C, 39.44; H, 3.63; N, 2.23; S, 5.09. Found: C, 39.85; H, 3.79; N, 2.12; S, 4.83.

{Cyclobis[(*cis*-(dppp)Pt(4-ethynylpyridyl)$_2$)(*cis*-(PEt$_3$)$_2$Pt)]Ag$_2$}$^{+6}$-(4,4′-dipyridylketone)($^-$OSO$_2$CF$_3$)$_6$ Complex (13). To a solution of silver triflate complex **5** in 750 μL of acetone-d_6 in a 5 mm NMR tube (39.0 mg, 0.0108 mmol) was added 1 equiv (2.0 mg, 0.0108 mmol) of 4,4′-dipyridyl ketone in one portion at 25 °C; then the reaction mixture was shaken. The solvent was removed under a stream of nitrogen at room temperature followed by solvent removal in vacuo, resulting in a yellow microcrystalline solid (40.8 mg, 99%): mp 175−180 °C dec; IR (CCl_4) 3051, 3098 (Ar), 2918 (CH_2), 2099 (CC), 1250, 1153, 1104, 1026 (OTf) cm^{-1}; ^{1}H NMR (acetone-d_6) δ 8.85 (d, 4H, $^3J_{HH}$ = 6.0 Hz, dipyridyl ketone-pyr-α), 8.73 (d, 8H), 7.79 (d, 4H, $^3J_{HH}$ = 6.0 Hz, dipyridyl ketone-pyr-β), 7.80−7.60 (m, 16H, *o*), 7.60−7.35 (m, 24H, *m*, *p*), 6.79 (d, 8H), 3.03 (bs, 8H), 2.20−1.85 (m, 8H), 2.10−1.80 (m, 24H), 1.50−1.10 (m, 36H); ^{13}C{^{1}H} NMR (acetone-d_6) δ 134.3 (Pt−P−C$_o$), 129.0 (Pt−P−C$_{ipso}$), 132.2 (Pt−P−C$_p$), 129.6 (Pt−P−C$_m$), 150.4 (C$_{\alpha pyr}$), 135.4 (C$_{ipsopyr}$), 130.2 (C$_{\beta pyr}$), 194.7 (dipyridyl ketone-CO), 152.1 (dipyridyl ketone-pyr-α), 143.7 (dipyridyl ketone-pyr-*ipso*), 124.2 (dipyridyl ketone-pyr-β), 108.8 (t, CC−Pt$_\beta$), 122.3 (q, J_{C-F} = 322 Hz, OTf), 23.9 (m, Pt−P−CH_2), 19.8 (bs, CH_2), 15.5 (m, Pt−P−CH_2CH_3), 8.2 (bs, Pt−P−CH_2CH_3); ^{31}P{^{1}H} NMR (acetone-d_6) δ 3.6 (s, J_{Pt-P} = 3075 Hz), −4.1 (s, J_{Pt-P} = 2294 Hz);^{19}F NMR (acetone-d_6) δ −75.

{Cyclobis[(*cis*-(dppp)Pt(4-ethynylpyridyl)$_2$)(*cis*-(PEt$_3$)$_2$Pd)]Ag$_2$}$^{+6}$-(pyrazine)($^-$OSO$_2$CF$_3$)$_6$ Complex (14). To a solution of silver triflate complex **6**[15] in 750 μL of acetone-d_6 in a 5 mm NMR tube (37.5 mg, 0.0110 mmol) was added 1 equiv (0.88 mg, 0.0110 mmol) of phenazine in one portion at 25 °C; then the reaction mixture was shaken. The solvent was removed under a stream of nitrogen at room temperature followed by solvent removal in vacuo, resulting in a yellow microcrystalline solid (38.1 mg, 99%): mp 210−214 °C dec; IR (CCl_4) 3051, 3098 (Ar), 2970 (CH_2), 2079 (CC), 1256, 1161, 1104, 1029 (OTf) cm^{-1}; ^{1}H NMR (acetone-d_6) δ 8.70 (d, 8H), 8.32 (d, 4H, pyrazine), 7.80−7.65 (m, 16H, *o*), 7.60−7.30 (m, 24H, *m*, *p*), 6.79 (d, 8H), 3.05 (bs, 8H), 2.25−1.95 (obscured m, 8H), 2.00−1.80 (m, 24H), 1.45−1.20 (m, 36H); ^{13}C{^{1}H} NMR (acetone-d_6) δ 134.4 (Pt−P−C$_o$), 130.0 (Pt−P−C$_{ipso}$), 132.4 (Pt−P−C$_p$), 129.7 (Pt−P−C$_m$), 150.5 (C$_{\alpha pyr}$), 129.0 (C$_{\beta pyr}$), 136.9 (C$_{ipsopyr}$), 146.9 (pyrazine), 109.0 (m, CC−Pt$_\beta$), 122.3 (q,

J_{C-F} = 320 Hz, OTf), 23.8 (m, Pt−P−CH_2), 19.8 (bs, CH_2), 16.5 (m, Pd−P−CH_2CH_3), 8.4 (bs, Pd−P−CH_2CH_3); $^{31}P\{^1H\}$ NMR (acetone-d_6) δ −4.5 (s, J_{Pt-P} = 2332 Hz), 31.7 (s); ^{19}F NMR (acetone-d_6) δ −75. Anal. Calcd for $Pt_2Pd_2Ag_2C_{116}H_{132}P_8S_6N_6O_{18}F_{18}\cdot OC(CD_3)_2$: C, 40.11; H, 4.07; N, 2.36; S, 5.40. Found: C, 40.43; H, 3.84; N, 2.19; S, 5.11.

{Cyclobis[(*cis*-(dppp)Pt(4-ethynylpyridyl)$_2$)(*cis*-(PEt$_3$)$_2$Pd)]Ag$_2$}$^{+6}$-(phenazine)($^-$OSO$_2$CF$_3$)$_6$ Complex (15). To a solution of silver triflate complex **6**[15] in 750 μL of acetone-d_6 in a 5 mm NMR tube (37.5 mg, 0.0110 mmol) was added 1 equiv (1.98 mg, 0.0110 mmol) of phenazine in one portion at 25 °C; then the reaction mixture was shaken. The solvent was removed under a stream of nitrogen at room temperature followed by solvent removal in vacuo, resulting in a yellow microcrystalline solid (39.3 mg, 99%): mp 188−191 °C dec; IR (CCl_4) 3056, 3093 (Ar), 2939 (CH_2), 2090 (CC), 1258, 1151, 1105, 1028 (OTf) cm^{-1}; ^1H NMR (acetone-d_6) δ 8.55 (d, 8H, $^3J_{HH}$ = 4.6 Hz), 8.47 (m, 4H, $^3J_{HH}$ = 10.0 Hz, phenazine-β), 8.03 (m, 4H, $^3J_{HH}$ = 10.0 Hz, phenazine-γ), 7.80−7.65 (m, 16H, *o*), 7.50−7.35 (m, 24H, *m*, *p*), 6.79 (d, 8H, $^3J_{HH}$ = 6.1 Hz), 3.10 (bs, 8H), 2.25−1.95 (obscured m, 8H), 1.95−1.87 (m, 24H), 1.40−1.20 (m, 36H); $^{13}C\{^1H\}$ NMR (acetone-d_6) δ 134.5 (Pt−P−C_o), 130.3 (Pt−P−C_{ipso}), 132.2 (Pt−P−C_p), 129.6 (Pt−P−C_m), 150.2 ($C_{\alpha pyr}$), 128.8 ($C_{\beta pyr}$), 137.2 ($C_{ipsopyr}$), 143.4 (phenazine-α), 133.1 (phenazine-β), 130.0 (phenazine-γ), 110.1 (m, CC−Pt_β), 122.3 (q, J_{C-F} = 321 Hz, OTf), 23.9 (m, Pt−P−CH_2), 19.8 (bs, CH_2), 16.3 (m, Pd−P−CH_2CH_3), 8.4 (bs, Pd−P−CH_2CH_3); $^{31}P\{^1H\}$ NMR (acetone-d_6) δ −4.0 (s, J_{Pt-P} = 2323 Hz), 31.4 (s); ^{19}F NMR (acetone-d_6) δ −75.

Acknowledgment. This article is dedicated to Professor Emanuel Vogel on the occasion of his 70th birthday. Financial support by the NSF (CHE-9529093, CHE-9002690), NIH (GM57052), and University of Utah Institutional Funds Committee and the generous loan of platinum(II) dichloride from Johnson-Matthey are gratefully acknowledged. The authors thank Dr. Bogdan Olenyuk and Dr. Stefan Leininger for assistance in computer modeling.

Supporting Information Available: Figures of the mass spectrum of **5**, a space-filling model, stacking diagram, and tables of positional parameters and esd's, anistropic displacement parameters, and an extended list of bond lengths and bond angles for compound **12** are available (20 pages). Ordering information is given on any current masthead page.

IC980727C